Ionic Conductivity of Gd- and Y-Doped Ceria-Zirconia Solid Solutions

Vera Rührup and Hans-Dieter Wiemhöfer

University of Münster, Institute of Inorganic and Analytical Chemistry, D-48149 Münster, Germany

Reprint requests to Prof. Dr. H.-D. Wiemhöfer. E-mail: hdw@uni-muenster.de.
Fax: +49 251 83 33193

Z. Naturforsch. **61b,** 916 – 922 (2006); received April 24, 2006

Dedicated to Professor Wolfgang Jeitschko on the occasion of his 70th birthday

The total conductivity of the solid solutions $(Ce_{1-x}Zr_x)_{0.8}Gd_{0.2}O_{1.9}$ and $(Ce_{1-x}Zr_x)_{0.8}Y_{0.2}O_{1.9}$ was measured in air as a function of temperature (T = 300 °C – 600 °C) and composition ($x = 0.0$ – 0.9). A deep minimum of the bulk ionic conductivity was found for equal fractions of ceria and zirconia. It indicates enhanced defect association and ordering of the oxygen vacancies around $x = 0.5$. X-ray analysis (Guinier technique) showed the diffraction pattern of the cubic fluorite structure for all investigated compositions $0 < x < 1$. The lattice parameter decreased linearly with increasing zirconia content x.

Key words: Ceria, Zirconia, Lattice Parameter, Ionic Conductivity, Impedance

Introduction

Ceria and zirconia doped by trivalent cations are well known solid electrolytes with high oxygen ion conductivity which makes them useful for solid oxide fuel cells or oxygen gauges. Doped ceria shows a somewhat higher oxygen ion conductivity than equally doped zirconia, but also a higher electronic conductivity. The latter prevents its application as solid electrolyte at temperatures well above 800 °C.

On the other hand, together with the oxygen ion conductivity, the redox activity of the Ce^{3+}/Ce^{4+} couple which also causes the higher *n*-type electron conduction compared to zirconia admits a fast reversible emission and storage of oxygen at elevated temperatures. Therefore, ceria is widely used as a fast oxygen storage component and redox mediator in heterogeneous catalysts [1]. A remarkable feature is that the substitution of half of the cerium ions by zirconium ions increases the oxygen storage capacity considerably [1 – 4]. Therefore, in the past years, ceria-zirconia solid solution systems have replaced pure ceria as oxygen storage compounds in catalysis. Many investigations have been carried out in order to clarify the role of zirconia in ceria-zirconia solid solutions for enhancing the reversible oxygen uptake. The presence of Zr^{4+} ions enhances the stability of Ce^{3+} ions and hence the reducibility of Ce^{4+} ions [2, 3]. It is supposed that the enhanced reducibility of ceria is closely connected with an easier formation of defect associates of Ce^{3+} and $V_O^{\cdot\cdot}$, probably with participation of Zr^{4+} cations [2, 4 – 6]. It is evident that an increase of vacancy association should be well discernible in the oxygen ion conductivity.

Analogously to the binary oxides, the oxygen ion conductivity of doped ceria-zirconia solid solutions is increased by doping with trivalent cations such as Y^{3+} and Gd^{3+}. This together with the enhanced electronic conductivity has aroused the interest in further applications based on the mixed ionic-electronic conductivity of ceria-zirconia solid solutions, for instance in electrodes [7] or oxygen separation membranes [8]. Up to now, only a few systematic investigations were carried out on the influence of the relative zirconia content on the ionic conductivity of ceria-zirconia systems doped with trivalent cations [9 – 12]. Ananthapadmanabhan *et al.* found a minimum of the total conductivity for $(Ce_{1-x}Zr_x)_{0.82}Y_{0.18}O_{1.91}$ at $x = 0.5$ [9]. They confirmed oxygen ions as majority charge carriers by EMF-measurements. Lee *et al.* investigated the influence of ceria-doping on the conductivity of yttria-stabilized zirconia (YSZ) [10]. Their results show for the zirconia rich systems $(Ce_{1-x}Zr_x)_{0.85}Y_{0.15}O_{1.925}$ ($x = 0.5 – 1$) an increase of conductivity with decreasing Ce-fraction. Huang *et al.* investigated the ionic conductivity of the ceria rich systems

$(Ce_{0.83}Sm_{0.17})_{1-x}Zr_xO_{2-\delta}$ ($x = 0-0.5$) and found a decrease for $x = 0-0.3$ and a slight increase for $x = 0.4$ and 0.5 [11]. Tsoga *et al.* prepared solid solutions by mixing and reacting $Ce_{0.8}Gd_{0.2}O_{1.9}$ (CGO) and $Zr_{0.85}Y_{0.15}O_{1.9}$ (YSZ) varying the composition x in the solid solutions $(YSZ)_x(CGO)_{1-x}$ [12]. They observed a minimum of the total conductivity around $x = 0.5$.

In this study we investigated the influence of the zirconia content x in $(Ce_{1-x}Zr_x)_{0.8}Gd_{0.2}O_{1.9}$ and $(Ce_{1-x}Zr_x)_{0.8}Y_{0.2}O_{1.9}$ on the oxygen ion conductivity. The constant, high dopant level of the trivalent Gd^{3+} or Y^{3+} causes a constant concentration of oxygen vacancies as long as the electron and hole concentrations remain small. The latter condition is fulfilled as shown by the data available for the electronic conductivities [10, 11]. Therefore, the total conductivity virtually corresponds to the oxygen ion conductivity, and hence will be a good monitor for changes of the oxygen vacancy mobility due to vacancy association or of the concentration of free vacancies in doped ceria-zirconia solid solutions as a function of x.

Experimental Section

Sample preparation

The samples $(Ce_{1-x}Zr_x)_{0.8}Gd_{0.2}O_{1.9}$ and $(Ce_{1-x}Zr_x)_{0.8}Y_{0.2}O_{1.9}$ ($x = 0.1-0.9$) were prepared by a solid state reaction using CeO_2, ZrO_2, Gd_2O_3 and Y_2O_3 (Chempur, 99.9%). Powders were mixed for 24 h by ball-milling with zirconia balls and ethanol as solvent. The resulting mixture was dried first at 50 °C for 24 h and afterwards at 100 °C for 2 h. Then, it was uniaxially pressed to pellets at 3.5 kbar and cold-isostatically condensed at 240 kbar [KIP 100 ES-PRESSYS, Weber]. The obtained pellets were sintered in air at 1600°C for 10 h. The final relative densities were $\geq 95\%$ of the theoretical densities (as determined from the unit cell volumes) for all samples.

X-ray diffraction

X-ray diffraction was used to check for phase purity and to determine the lattice parameters. A Guinier camera (Enraf – Nonius, type Fr 552) with Cu-K_α-radiation and an image plate detector system (Fujifilm) were used. The positions and intensities were read out using a BAS 1800-Scanner. The lattice parameters were calculated using the software "Win-XPOW" [13].

Total conductivity

The sintered ceramic pellets were covered with porous platinum paste contacts (Degussa-Hüls 6402 1001). Impedance spectra were recorded in air using a frequency response analyzer (Solartron 1260) in the frequency range 0.1 Hz – 1 MHz. The impedance data were evaluated in terms of suitable equivalent circuits using the ZView software package (Scribner Associates). The total conductivities were obtained in the temperature range 300 to 600 °C. At temperatures below 600 °C, the appearance of a second time constant (additional arc in the complex plane plot) indicated the presence of a grain boundary impedance. Hence, bulk and grain boundary conductivities were separately evaluated at the lower temperatures assuming that both are in series.

Table 1. Cation radii according to [16].

Ion	Radius (nm)	Ion	Radius (nm)
Ce^{4+}	0.097	Zr^{4+}	0.084
Gd^{3+}	0.105	Y^{3+}	0.102

Results and Discussion

Phase composition

All samples showed the diffraction pattern of the cubic fluorite structure only. No indications for the occurrence of a second phase were found in any of the samples. The lattice parameters could be evaluated with high accuracy. Results are shown in Fig. 1, where the lattice parameters are plotted *versus* the zirconia content x. For both dopants, there is a linear decrease with increasing Zr content according to the relations

$$(Ce_{1-x}Zr_x)_{0.8}Gd_{0.2}O_{1.9}, 20\ ^\circ C: \quad a\,[nm] = 0.5413 - 0.0245 \cdot x \tag{1}$$

$$(Ce_{1-x}Zr_x)_{0.8}Y_{0.2}O_{1.9}, 20\ ^\circ C: \quad a\,[nm] = 0.5393 - 0.0244 \cdot x \tag{2}$$

The overall change of the lattice parameter is explained by the difference of the cation radii of cerium and zirconium (*cf.* Table 1). Taking into account the experimental accuracy, the deviation from Vegard's law is negligible in Fig. 1. The results for the Y-doped systems are in good agreement with literature data. Calés and Baumard determined a [nm] = $(0.5388 - 0.0243 \cdot x)$ for samples with slightly different dopant concentrations, *i.e.* $(Ce_{1-x}Zr_x)_{0.82}Y_{0.18}O_{1.91}$ [14]. Ananthapadmanabhan *et al.* found a [nm] = $(0.5400 - 0.0264 \cdot x)$ for the same compositions as investigated by Calés and Baumard [9]. Concerning the Gd-doped analogues, very few data are available. Grover *et al.* investigated phases and lattice parameters of a few compositions in the CeO_2-Gd_2O_3-ZrO_2 system [15]. Table 2 compiles lattice parameters of Gd-doped materials as de-

Table 2. Lattice parameters of the system $(Ce_{1-x}Zr_x)_{0.8}Gd_{0.2}O_{1.9}$ at r. t. in comparison with literature data.

	Lattice parameter (nm)	Literature
$Ce_{0.8}Gd_{0.2}O_{1.9}$	0.5418 ± 0.0001	0.5422 [12] 0.5417 [18]
$(Ce_{0.9}Zr_{0.1})_{0.8}Gd_{0.2}O_{1.9}$	0.5390 ± 0.0001	
$(Ce_{0.8}Zr_{0.2})_{0.8}Gd_{0.2}O_{1.9}$	0.5365 ± 0.0002	0.5388 [15]
$(Ce_{0.7}Zr_{0.3})_{0.8}Gd_{0.2}O_{1.9}$	0.5331 ± 0.0002	
$(Ce_{0.6}Zr_{0.4})_{0.8}Gd_{0.2}O_{1.9}$	0.5308 ± 0.0001	
$(Ce_{0.5}Zr_{0.5})_{0.8}Gd_{0.2}O_{1.9}$	0.5295 ± 0.0002	0.5294 [15]
$(Ce_{0.3}Zr_{0.7})_{0.8}Gd_{0.2}O_{1.9}$	0.5244 ± 0.0002	
$(Ce_{0.1}Zr_{0.9})_{0.8}Gd_{0.2}O_{1.9}$	0.5193 ± 0.0003	

Table 3. Lattice parameters of $(Ce_{1-x}Zr_x)_{0.8}Y_{0.2}O_{1.9}$ in comparison with literature data.

	Lattice parameter (nm)	Literature
$Ce_{0.8}Y_{0.2}O_{1.9}$	0.5404 ± 0.0001	0.5410 [19] 0.5405 [20]
$(Ce_{0.9}Zr_{0.1})_{0.8}Y_{0.2}O_{1.9}$	0.5365 ± 0.0002	0.5381 [20]
$(Ce_{0.8}Zr_{0.2})_{0.8}Y_{0.2}O_{1.9}$	0.5341 ± 0.0002	0.5355 [20]
$(Ce_{0.7}Zr_{0.3})_{0.8}Y_{0.2}O_{1.9}$	0.5316 ± 0.0002	0.5328 [20]
$(Ce_{0.6}Zr_{0.4})_{0.8}Y_{0.2}O_{1.9}$	0.5293 ± 0.0001	0.5302 [20]
$(Ce_{0.5}Zr_{0.5})_{0.8}Y_{0.2}O_{1.9}$	0.5271 ± 0.0003	0.5275 [20]
$(Ce_{0.3}Zr_{0.7})_{0.8}Y_{0.2}O_{1.9}$	0.5225 ± 0.0002	0.5223 [20]
$(Ce_{0.1}Zr_{0.9})_{0.8}Y_{0.2}O_{1.9}$	0.5176 ± 0.0004	0.5173 [20]

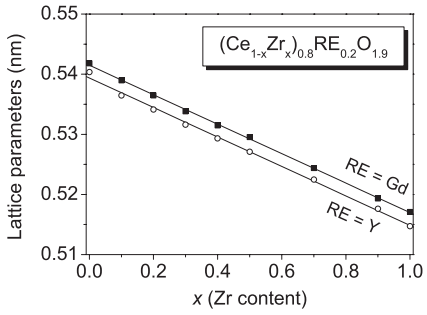

Fig. 1. Lattice parameters of $(Ce_{1-x}Zr_x)_{0.8}RE_{0.2}O_{1.9}$ for RE = Gd and Y as a function of the composition x at r. t. Lattice parameters of $Zr_{0.8}Gd_{0.8}O_{1.9}$ and $Zr_{0.8}Y_{0.8}O_{1.9}$ are taken from [15, 17].

termined in this work in comparison with some results of Grover.

Ionic conductivity

Fig. 2 shows a complex plane plot of the impedance results with two semicircles at 450 °C. This result is typical for temperatures below 600 °C. Basically, the two semicircles are explainable by a series circuit of a bulk and a grain boundary impedance. The higher frequency semicircle corresponds to the bulk impedance consisting of a parallel circuit of the bulk resistance R_{bulk} and a constant phase element CPE_{bulk}. The semi-

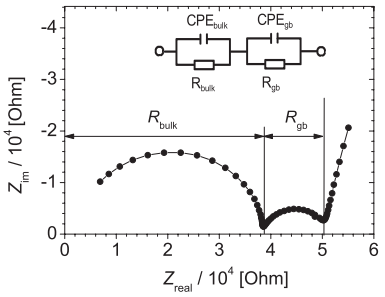

Fig. 2. Impedance plot of the cell Pt (air) | $(Ce_{0.5}Zr_{0.5})_{0.8}Y_{0.2}O_{1.9}$ | Pt(air) at 450 °C. (Parameters: $R_{bulk} = 3.70 \cdot 10^4$ Ohm, $R_{gb} = 1.11 \cdot 10^4$ Ohm, $CPE_{bulk} = 5.89 \cdot 10^{-11}$ F, $CPE_{gb} = 1.42 \cdot 10^{-7}$ F).

circle at lower frequencies is due to a grain boundary impedance which consists of the grain boundary resistance R_{gb} and a parallel constant phase element CPE_{gb}. Both constant phase elements nearly correspond to a capacitance. Accordingly, the net total resistance R_{total} consists of the sum of the bulk and the grain boundary resistance as given by

$$R_{total} = R_{bulk} + R_{gb} \tag{3}$$

The separate contributions of bulk and grain boundaries could be distinguished up to temperatures around 600 °C. Above that temperature, no separate grain boundary contribution could be distinguished. Applying the same cell constant (l/A, with pellet thickness l and electrode surface area A), the bulk and the grain boundary conductivities were calculated according to

$$\sigma_{bulk} = \frac{l}{A} \cdot \frac{1}{R_{bulk}}, \quad \sigma_{gb} = \frac{l}{A} \cdot \frac{1}{R_{gb}} \tag{4}$$

Even in the cases of $(Ce_{0.5}Zr_{0.5})_{0.8}Gd_{0.2}O_{1.9}$ and $(Ce_{0.5}Zr_{0.5})_{0.8}Y_{0.2}O_{1.9}$, the systems with the lowest total conductivity, the measured total conductivities are more than two orders of magnitude higher than the electronic conductivities (in air). For instance, $(Ce_{0.5}Zr_{0.5})_{0.8}Gd_{0.2}O_{1.9}$ showed $\sigma_{bulk}(600\,°C) = 2.7 \cdot 10^{-4}$ S/cm, whereas the electronic conductivity was $\sigma_{electron}(600\,°C) \approx 10^{-6}$ S/cm in air [21]. Therefore, the total conductivities measured in air are virtually equal to the oxygen ion conductivities and the electronic conductivities are negligible.

Figs 3a and 3b show the bulk and grain boundary conductivities for two samples with the compositions $(Ce_{0.5}Zr_{0.5})_{0.8}Gd_{0.2}O_{1.9}$ and $(Ce_{0.5}Zr_{0.5})_{0.8}Y_{0.2}O_{1.9}$.

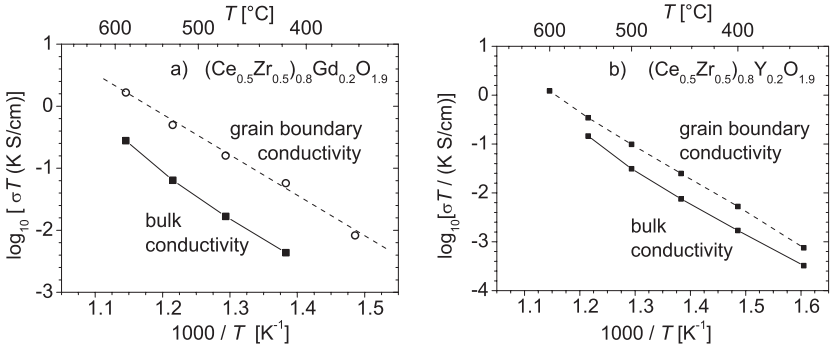

Fig. 3. Bulk and grain boundary conductivities a) of $(Ce_{0.5}Zr_{0.5})_{0.8}Gd_{0.2}O_{1.9}$ and b) of $(Ce_{0.5}Zr_{0.5})_{0.8}Y_{0.2}O_{1.9}$.

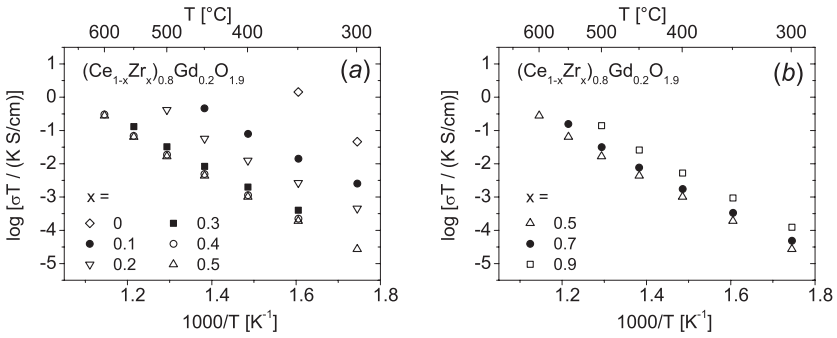

Fig. 4. Temperature dependence of the bulk conductivities of the $(Ce_{1-x}Zr_x)_{0.8}Gd_{0.2}O_{1.9}$ solid solutions: a) $x = 0.0 - 0.5$; b) $x = 0.5 - 0.9$.

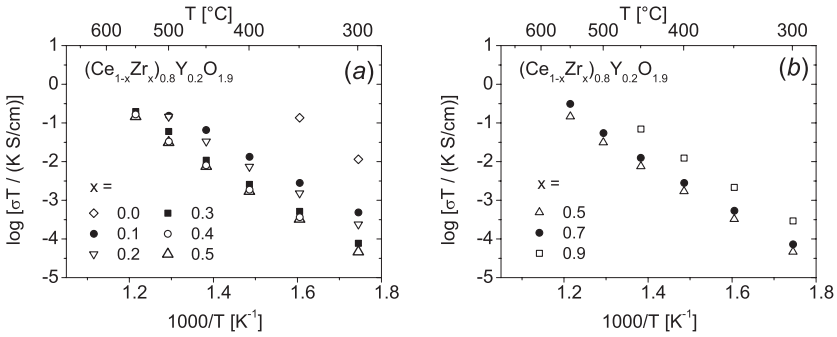

Fig. 5. Temperature dependence of the bulk conductivities of the $(Ce_{1-x}Zr_x)_{0.8}Y_{0.2}O_{1.9}$ solid solutions: a) $x = 0.0 - 0.5$; b) $x = 0.5 - 0.9$.

The grain boundary conductivities are about one order of magnitude higher than the bulk conductivities and follow a perfect linear relationship in the Arrhenius diagrams. The bulk conductivities in Fig. 3, however, show a slight curvature with increasing slope towards higher temperatures. The results for the bulk conductivities as shown in both parts of Fig. 3 compare well with literature data for the analogous system $(Ce_{0.5}Zr_{0.5})_{0.8}Sm_{0.2}O_{1.9}$ [11].

Figs 4 and 5 show the conductivities of $(Ce_{1-x}Zr_x)_{0.8}RE_{0.2}O_{1.9}$ with RE = Gd and Y as a function of temperature. For clarity, the results for compositions above and below $x = 0.5$ are plotted in separate diagrams. One observes a strong dependence of the oxygen ion conductivity on the composition x in both solid solutions. For instance, the bulk conductivity of $(Ce_{0.9}Zr_{0.1})_{0.8}Gd_{0.2}O_{1.9}$ is about two orders of magnitude higher than that of $(Ce_{0.5}Zr_{0.5})_{0.8}Gd_{0.2}O_{1.9}$ which exhibits the lowest ionic conductivity (Fig. 4). The same can be observed in the Y-doped solid solutions (Fig. 5), even though the differences are somewhat smaller there. Plots of the grain boundary conductivity which are not shown here in principle exhibit the same behaviour, but the variation is higher.

A direct comparison of Gd- and Y-doped samples at a constant temperature of 400 °C is shown in Fig. 6. A clear minimum of the conductivities is seen for both systems at $x = 0.5$. The conductivity decrease amounts to more than two orders of magnitude as compared to doped ceria, *i.e.* $x = 0$, and at least one order of

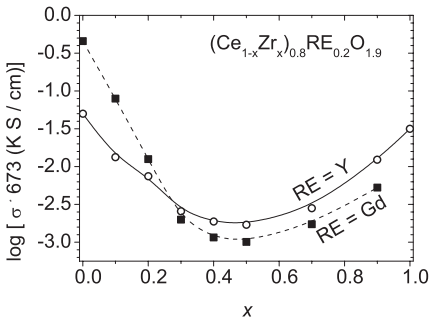

Fig. 6. Bulk conductivity of $(Ce_{1-x}Zr_x)_{0.8}(Gd/Y)_{0.2}O_{1.9}$ at 400 °C. The data points at $x = 0.0$ and $x = 1.0$ for the Y-doped samples (RE = Y) were taken from [29] and [25] respectively. No data were available at 400 °C for the composition $Zr_{0.8}Gd_{0.2}O_{1.9}$.

magnitude as compared to stabilized zirconia. In view of the constant concentration of the trivalent dopants and hence of the oxygen vacancies, such a strong dependence is surprising. The results indicate a distinctive association and local ordering of oxygen vacancies around $x = 0.5$.

Many authors have studied and discussed association and ordering of oxygen vacancies for ceria as well as for zirconia as a function of the kind of dopant ion and/or as a function of the dopant concentration with respect to an optimum of the oxygen ion conductivity [22 – 27]. In our systems, the dopant concentrations are constant. Hence, the changes of the association and local ordering of oxygen vacancies observed here are a function of the ratio of zirconia to ceria reaching a maximum near the ratio 1 : 1. This is probably closely connected to the enhanced reducibility of ceria-zirconia solid solutions [28].

In agreement with results for Y- and Gd-doped zirconia [25], Y-doped ceria-zirconia samples show higher conductivities at zirconia-rich compositions. On the other hand, similarly and in agreement with results for Y- and Gd-doped ceria in the literature [26, 27], the ceria-rich systems $(Ce_{1-x}Zr_x)_{0.8}Gd_{0.2}O_{1.9}$ with $x = 0.0 – 0.2$ show higher conductivities as compared to the Y-doped materials with the same ceria-zirconia ratio. A crossover is observed between $x = 0.2$ and $x = 0.3$. Therefore, the behaviour of the dopant ions is analogous to that in pure doped zirconia or ceria systems and mainly caused by the ratio of the corresponding cation radii (*cf.* Table 1). The maximum of ionic conductivity of ceria occurs with Gd-doping which is explained by the minimum of the association enthalpy of Gd^{3+} and $V_O^{\cdot\cdot}$ and the optimum ratio of the cation radii of Ce^{4+} and Gd^{3+}. An analogous explanation for the difference in oxygen ion conductivity is given for zirconia with regard to the dopant effects of Y^{3+} and Gd^{3+}.

The activation energies derived from the temperature dependent bulk conductivities of this work are shown in Fig. 7a. It is evident that the ceria-zirconia solid solutions show a broad maximum of the activation energies. The values are nearly 0.4 to 0.5 eV higher as compared to Gd-doped ceria or Y-doped zirconia alone. There is agreement between many authors that the activation energy as determined from the temperature dependent oxygen ion conductivity for doped zirconia and ceria systems consists of the migration enthalpy ΔH_m and an association enthalpy ΔH_a which mainly involves the association equilibrium of vacancies and trivalent ions.

$$E_{A,bulk} = \Delta H_m + \Delta H_a \tag{5}$$

Hence within this model, the association term contains the specific properties of the various dopants. According to [29], for Gd-doped ceria, the association term is -0.18 eV and for Y-doped ceria -0.39 eV. Values for the corresponding Y- or Gd-doped zirconia are available predominantly for high temperatures and therefore are not so well comparable. For instance, at 1000 °C, Gd-doped zirconia gave an association enthalpy ΔH_a of -0.62 eV and Y-doped zirconia of -0.39 eV. For the ceria-zirconia solid solutions, the association equilibria are complicated by the presence of a varying concentration of cerium and zirconium ions which gives rise to additional possible defect complexes with a local ordering of cerium, zirconium and the dopant ions in the vicinity of the vacancies. The migration enthalpy of oxygen ions in pure doped ceria or zirconia alone lies in the range 0.7 to 0.8 eV [25, 29].

In ceria-zirconia solid solutions, however, the situation is not as simple. The maximum of the activation energy may at least partially be due to a maximum of the migration enthalpy, because the unsymmetrical occupation of the structure by three types of cations leads to variable local energy barriers around a vacancy site. The different cation radii of cerium and zirconium and the effect of local strain may lead to different site energies for vacancies. These differences in site energy will cause an increased local ordering and restrictions for the possible oxygen jumps.

Only a few data are available in the literature for the variation of activation energies of ceria-

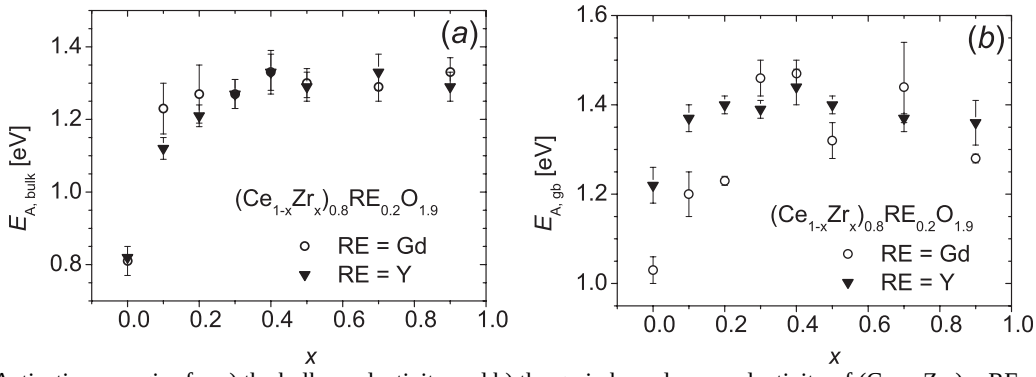

Fig. 7. Activation energies for a) the bulk conductivity and b) the grain boundary conductivity of $(Ce_{1-x}Zr_x)_{0.8}RE_{0.2}O_{1.9}$.

Table 4. Activation energies from the literature for the total conductivity for some comparable ceria-zirconia solid solutions with similar compositions.

	$(Ce_{1-x}Zr_x)_{0.82}Y_{0.18}O_{1.91}$ [9]	$(Ce_{0.83}Sm_{0.17})_{1-x}Zr_xO_{2-\delta}$ [11]
$x = 0.0$	0.76 eV	0.85 eV
$x = 0.5$	1.23 eV	1.10 eV
$x = 1.0$	0.78 eV	–

zirconia solid solutions at constant dopant concentrations. Table 4 shows results from two investigations for $(Ce_{1-x}Zr_x)_{0.82}Y_{0.18}O_{1.91}$ and $(Ce_{0.83}Sm_{0.17})_{1-x}Zr_xO_{2-\delta}$ [9, 11]. It is evident that the general dependence of the activation energies is rather similar to the systems studied in this work.

Conclusions

Lattice parameters and bulk and grain boundary conductivities were investigated for the two solid solution series $(Ce_{1-x}Zr_x)_{0.8}Gd_{0.2}O_{1.9}$ and $(Ce_{1-x}Zr_x)_{0.8}Y_{0.2}O_{1.9}$ ($x = 0.0-0.9$).

All samples exhibited the cubic fluorite structure. An almost ideal linear relation between the lattice parameter and the relative change of the zirconia-content could be observed at constant concentration of the trivalent dopants.

As expected for systems with high ceria-content, the Gd-doped samples show the highest conductivities. On the other hand, for zirconia-rich systems, the Y-doped samples showed higher ionic conductivities than Gd-doped materials. This is in agreement with an interpolation of the behaviour of the boundary compositions (*i.e.* pure Gd- or Y-doped ceria and zirconia) at $x = 0.0$ and $x = 1.0$ and mainly follows the changes expected from the differences of the ionic radii of host and dopant ions.

The Gd- as well as the Y-doped systems exhibited a deep minimum of the ionic conductivity near a 1 : 1 ratio of Ce and Zr. This effect is independent of the kind of dopant. These observations are explainable by a strong association and ordering of the vacancies in local defect complexes probably accompanied by an increase of the mean migration enthalpy due to local strain.

Acknowledgements

We are grateful to R.-D. Hoffmann for his support in XRD analysis. We also thank the Deutsche Forschungsgemeinschaft (DFG) for the financial support of this work within the priority programm 1136 “Substitution effects in ionic solids”.

[1] J. Kaspar, P. Fornasiero, M. Graziani, Catalysis Today **50**, 285 (1999).
[2] G. Balducci, J. Kaspar, P. Fornasiero, M. Graziani, M. S. Islam, J. D. Gale, J. Phys. Chem. B **101**, 1750 (1997).
[3] P. Fornasiero, G. Balducci, R. Di Monte, J. Kaspar, V. Sergo, G. Gubitosa, A. Ferrero, M. Graziani, J. Catalysis **164**, 173 (1996).
[4] G. Balducci, M. S. Islam, J. Kaspar, P. Fornasiero, M. Graziani, Chem. Mater. **12**, 677 (2000).
[5] F. Esch, C. Africh, G. Comelli, R. Rosei, S. Fabris, L. Zhou, T. Montini, P. Fornasiero, Science **309**, 752 (2005).
[6] N. V. Skorodumova, S. I. Simak, B. I. Lundqvist, I. A. Abrikosov, B. Johansson, Phys. Rev. Lett. **89**, 166601/1 (2002).
[7] E. P. Murray, T. Tsai, S. A. Barnett, Nature (London) **400**, 649 (1999).
[8] Y. Nigara, K. Watanabe, K. Kawamura, J. Mizusaki, M. Ishigame, J. Electrochem. Soc. **144**, 1050 (1997).

[9] P. V. Ananthapadmanabhan, N. Venkatramani, V. K. Rohatgi, A. C. Momin, K. S. Venkateswarlu, J. Eur. Ceram. Soc. **6**, 111 (1990).
[10] C. H. Lee, G. M. Choi, Solid State Ionics **135**, 653 (2000).
[11] W. Huang, P. Shuk, M. Greenblatt, M. Croft, F. Chen, M. Liu, J. Electrochem. Soc. **147**, 4196 (2000).
[12] A. Tsoga, A. Naoumidis, D. Stöver, Solid State Ionics **135**, 403 (2000).
[13] Stoe & Cie, Win-XPow 1.09, Darmstadt (2002).
[14] B. Calès, J. F. Baumard, J. Electrochem. Soc. **131**, 2407 (1984).
[15] V. Grover, A. K. Tyagi, J. Solid State Chem. **177**, 4197 (2004).
[16] R. D. Shannon, Acta Crystallogr. **A32**, 751 (1976).
[17] M. Yashima, S. Sasaki, M. Kakihana, Y. Yamaguchi, H. Arashi, M. Yoshimura, Acta Crystallogr. **B51**, 381 (1995).
[18] N. M. Sammes, Z. Cai, Solid State Ionics **100**, 39 (1997).
[19] E. R. Andrievskaya, V. P. Red'ko, L. M. Lopato, Powder Metallurgy and Metal Ceramics (Translation of Poroshkovaya Metallurgiya (Kiev)) **40**, 405 (2002).
[20] N. Sakai, T. Hashimoto, T. Katsube, K. Yamaji, H. Negishi, T. Horita, H. Yokokawa, Y. P. Xiong, M. Nakagawa, Y. Takahashi, Solid State Ionics **143**, 151 (2001).
[21] V. Rührup, T. Bredow, H.-D. Wiemhöfer, in preparation.
[22] H. Yahiro, Y. Eguchi, K. Eguchi, H. Arai, J. Appl. Electrochem. **18**, 527 (1988).
[23] J. A. Kilner, Solid State Ionics **129**, 13 (2000).
[24] I. Kosacki, V. Petrovsky, H. U. Anderson, J. Electroceramics **4**, 243 (2000).
[25] Y. Arachi, H. Sakai, O. Yamamoto, Y. Takeda, N. Imanishai, Solid State Ionics **121**, 133 (1999).
[26] V. Butler, C. R. A. Catlow, B. E. F. Fender, J. H. Harding, Solid State Ionics **8**, 109 (1983).
[27] R. Gerhardt-Anderson, A. S. Nowick, Solid State Ionics **5**, 547 (1981).
[28] G. Balducci, J. Kaspar, P. Fornasiero, M. Graziani, M. S. Islam, J. Phys. Chem. B **102**, 557 (1998).
[29] H. Inaba, H. Tagawa, Solid State Ionics **83**, 1 (1996).